

Manifestations of the Indian Ocean tsunami of 2004 in satellite nadir-viewing radar backscatter variations

Yuliya I. Troitskaya¹ and Stanislav A. Ermakov¹

Received 22 August 2005; revised 3 January 2006; accepted 5 January 2006; published 24 February 2006.

[1] The paper reports on the first experimental evidence for space-observed manifestation of the open ocean tsunami in the microwave radar backscatter (in C- and Ku-bands; electromagnetic wave lengths 6cm and 2 cm respectively). Significant (a few dB) variations of the radar cross section synchronous with the sea level anomaly were found in the geophysical data record of the altimetry satellite Jason-1 for the track which crossed the head wave of the catastrophic tsunami of 26 December 2004. The simultaneous analysis of the available complementary data provided by the satellite three-channel radiometer enabled us to exclude meteorological factors as possible causes of the observed signal modulation. A possible physical mechanism of modulation of short wind waves due to transformation of the thin boundary layer in the air by a tsunami wave is discussed. The results open new possibilities of monitoring tsunamis from space. **Citation:** Troitskaya, Y. I., and S. A. Ermakov (2006), Manifestations of the Indian Ocean tsunami of 2004 in satellite nadir-viewing radar backscatter variations, *Geophys. Res. Lett.*, 33, L04607, doi:10.1029/2005GL024445.

1. Introduction

[2] The catastrophic tsunami of 26 December 2004 emphasized the need in a functioning global system of tsunami early warning. A space-borne system of tsunami monitoring would have been an ideal solution because of global coverage and instant access to the information. At present, the only known way of tsunami satellite remote sensing is via space-borne altimetry [see *Okal et al.*, 1999; *Zaychenko et al.*, 2004], which, unfortunately, is of limited practical value: to register a tsunami a satellite should be exactly above the wave in question. In this context, it would have been preferable to employ side-looking instruments providing large-scale panorama of the sea surface, for example, synthetic aperture radars. The key open question was, whether a tsunami can produce a signature at a radar image, that is, cause modulation of the short waves (“sea roughness”) sufficient for instrumental registration. Here we report on the first experimental evidence for space-observed manifestation of the open ocean tsunami in the microwave radar backscatter (in C- and Ku-bands).

[3] There are some reports on manifestations of the tsunami of 26 December in optical and infrared satellite imagery in the coastal zone, where the tsunami was strong enough and a noticeable effect of modulation the of “sea roughness” could be expected (see, e.g., http://www-misr.jpl.nasa.gov/gallery/galhistory/2005_jan_12.html, <http://crisp.nus.edu.sg/tsunami/tsunami.html>). Note that according to some earlier eyewitness observations [see *Godin*, 2004, and references therein], the so-called “tsunami shadow” occurs in the vicinity of the shore as a dark band along the tsunami front, presumably caused by modulation of wind waves. However, for the open ocean conditions, visibility of a tsunami was in question. The unique case of the huge tsunami of 26 December 2004 enables one to elucidate the situation.

[4] Unfortunately, neither radar, nor infrared or optical images of the tsunami on December 26, 2004 were acquired in the open ocean. At the same time, the satellite Jason-1 track crossed the head tsunami wave at 5°S 82°E at 2 h 53 min UTC, that is, 1 h 55 min after the earthquake (track 129 of cycle 109). The radar altimeter duly reliably registered the sea level displacements associated with the head tsunami wave and even its shape [see *Gower*, 2005; *Kulikov*, 2005], which was corroborated by numerical simulations [see *Scharroo et al.*, 2005; *Lay et al.*, 2005]. We checked, whether there are variations of received power of radio waves synchronous with the tsunami and associated with variations of the sea roughness. The radar cross section (RCS) is included in the geophysical data record (GDR) of Jason-1 [see *Picot et al.*, 2003] for the radar altimeter operating in C and Ku bands (electromagnetic wave lengths 6cm and 2 cm, respectively). The data collected by the Physical Oceanography Distributed Active Archive Center (PODAAC) are available online [anonymous ftp ftp://podaac.jpl.nasa.gov/pub/sea_surface_height/jason/gdr/]. Time series of the Sea Level Anomaly and C- and Ku-band RCS are presented in Figure 1a. The sea level variations due to the tsunami are clearly seen north of the latitude -5° , the surface displacements exceed 0.6m and the spatial scale of the wave is a few hundreds of km. RCS is seen to be varied significantly (a few dB) simultaneously with the sea level. Note that according to the wind velocity vector data obtained from the meteorological model of the European Center for Medium Range Weather Forecasting (ECMWF) and shown in (Figures 1b and 1c) (taken from GDR) the tsunami front near the equator passed an area of weak wind and our further analysis will be focused on this case.

2. Analysis of the GDR of Jason-1

[5] RCS variations associated with modulation of short wind waves by tsunami waves can be masked by variations due to other physical mechanisms, in particularly, due to some meteorological factors. To relate unambiguously the RCS variations in Figure 1 with the tsunami, below we analyze the GDR data in the latitude range -5° -5° (Figure 2a) and rule out some background meteorological

¹Institute of Applied Physics, Russian Academy of Sciences, Nizhny Novgorod, Russia.

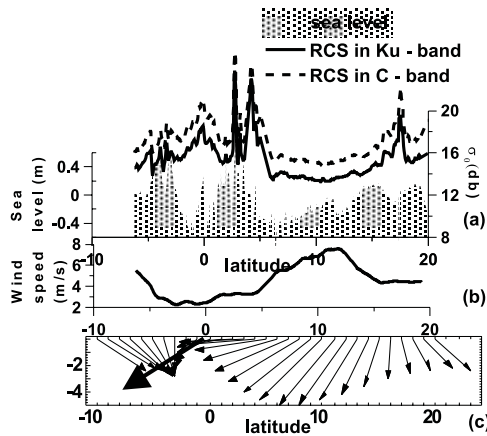


Figure 1. Latitude dependencies of parameters from the geophysical data record of the Jason-1 altimetry satellite 26 December 2004 (cycle 109, track 129) (a) sea level anomaly and C- and Ku-band RCS, (b) the 10 m wind speed and (c) the directions of wind speed (small arrows) according to the ECMWF model and the tsunami wave propagation (large arrow) near the equator according to numerical simulations [see *Scharroo et al.*, 2005; *Lay et al.*, 2005].

factors, including variations of wind speed and the total electron content (the latter retrieved is shown in Figure 2c).

[6] Measurements of the atmospheric conditions independent from the radar altimeter data aboard Jason-1 are provided by the 3-channel radiometer operating at frequencies 18.7 GHz, 23.8 GHz, 34 GHz, which are used for

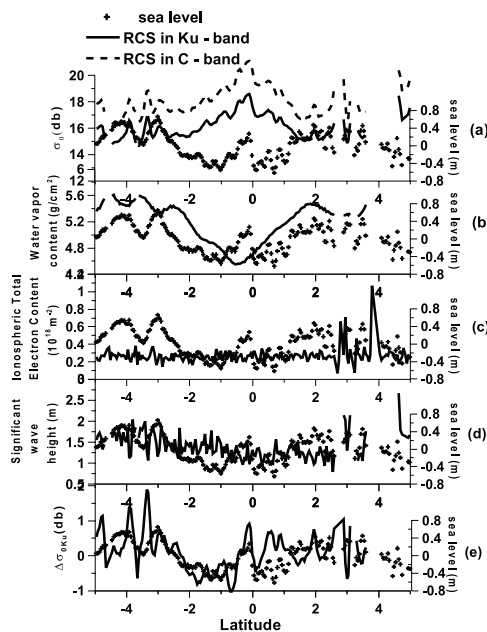


Figure 2. The enlarged segment of the record. (a) The sea level anomaly and RCS in C and Ku bands, (b) water vapor content (c) ionosphere total electron content, (d) the significant wave height, (e) fluctuations of the Ku-band RCS over background. The plot is discontinuous, where there are data, which do not meet data editing criteria [see *Picot et al.*, 2003].

retrieving water vapor content in the atmosphere (Figure 2b). The corresponding brightness temperatures also reflect the variations of the sea surface roughness, however, under the conditions of the weak wind, which occur in the domain $\pm 5^\circ$, the wind velocity cannot be reliably determined on the base of radiometry. We supposed that the water vapor content is independent on the sea level elevation in the tsunami wave and can be taken as a measure of background meteorological variations. We retrieved the empirical dependence of RCS on the water vapor content C_V from the GDR data taken within the range $\pm 5^\circ$ (Figure 3), which reflects the local weather conditions, the best fit for it is:

$$\langle \sigma_{0Ku} \rangle (C_V) = -3.18 C_V + 32.5 \quad (1)$$

[7] It is worth mentioning that the value of the significant wave height was about 1.5 m without strong fluctuations (Figure 2d), and large-scale variability correlated with the sea level elevation in the tsunami wave is not detected too.

[8] To rule out the meteorological factor we considered the value

$$\Delta \sigma_{0Ku} = \sigma_{0Ku} - \langle \sigma_{0Ku} \rangle (C_V)$$

The along track section of $\Delta \sigma_{0Ku}$ is presented in Figure 2e. The cloud of points $\Delta \sigma_{0Ku}$ via the sea level anomaly (Figure 4) demonstrates significant correlation among these two values. The correlation coefficient is about 0.5 in the range $-5^\circ \div 2.5^\circ$, where there is no significant fluctuations of the electron content in the ionosphere (see Figure 2c), and it is about 0.65 in the range $-5^\circ \div 0^\circ$, where the sea level anomaly is reliably interpreted as the tsunami wave according to *Scharroo et al.* [2005] and *Lay et al.* [2005].

3. Possible Mechanism of Modulation of Surface Waves in the Presence of the Tsunami Wave

[9] Mechanisms of modulation of short wind waves responsible for the scattering properties of the sea surface in the presence of an inhomogeneous unsteady flow caused by tsunami are unknown. Those previously developed to describe similar modulation in the context of internal waves [see, e.g., *Alpers*, 1985] as a result of straining of surface waves prove to be practically negligible. The following possible physical mechanism seems to be the most likely candidate, at least at low wind, to explain the effect of a tsunami on short surface waves. The orbital velocities of the tsunami wave cause modulation of wind velocity over the sea surface [see *Godin*, 2004]. This results in the modula-

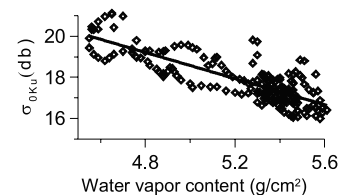


Figure 3. Ku-band RCS via 23.8 GHz brightness temperature near the equator for 129 track. The solid line is the best-fit line given by equation (1).

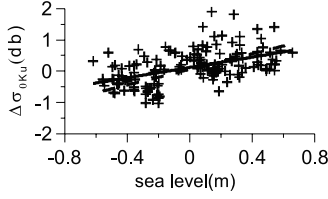


Figure 4. Dependence of $\Delta\sigma_{0k_u}$ on the sea level elevation (points). The solid line is the best fit for points between -5° and 2.5° (correlation coefficient is 0.49), the dashed line is the best fit for points between -5° and 0° (correlation coefficient is 0.65).

tion of the surface wave growth rate that in turn causes variations of the intensity of short surface waves. This mechanism was earlier discussed in detail in the context of radar probing of long surface waves and swell in the papers by *Kudryavtsev et al.* [1997] and *Troitskaya* [1994] and is used below to estimate the RCS variations due to tsunami [Godin, 2004]. It should be mentioned, that natural variations in wind field are much stronger than the tsunami induced velocity. Fortunately, the spatial scale of such variations is about 1 km, and it is averaged due to the spatial resolution of the altimeter at 1 Hz measurements; taking into account the ground track speed for Jason-1, 5.8 km/s [see *Picot et al.*, 2003] gives resolution about 6 km. We estimated hydrodynamic contrast caused by the tsunami wave in the field of surface wind waves, basing on the models by *Kudryavtsev et al.* [1997] and *Troitskaya* [1994]. It is worth mentioning, that nonlinear wave-wind interaction, i.e., modulation of the roughness parameter, should be taken into account [see *Kudryavtsev et al.*, 1997]. To describe disturbances induced in the air by the tsunami wave, we employ the model of the atmospheric boundary layer over the waved water surface developed by *Reutov and Troitskaya* [1995], which includes the Reynolds equations closed on the base of the gradient approximation of turbulent stresses. The system of equations for the disturbance induced in the air by the tsunami wave can be reduced to the diffusion equation for the horizontal velocity:

$$\partial_t U = \partial_\eta (\nu_t \partial_\eta U) - \partial_\eta \tau_{wave} \quad (2a)$$

$$U|_{\eta=0} = U_w(t-x/c)U|_{\eta \rightarrow \infty} = u_{*0}/\kappa \ln \eta/z_0 \quad (2b)$$

Here τ_{wave} – is the wind wave stress, $U_w(t-x/c)$ is the orbital velocity of the tsunami wave, $c = \sqrt{gH}$ is the tsunami wave velocity, u_{*0} is the wind friction velocity; z_0 is the roughness parameter. The coordinate line $\eta = 0$ coincides with the water surface bended by the tsunami wave. Since wind flow over the water surface is hydrodynamically smooth for the case of weak winds [see, e.g., *Miles*, 1962], we used the expression for ν_t obtained on the base of experiments with the turbulent boundary layer over a smooth plane by *Smolyakov* [1973]:

$$\nu_t(z) = \nu_a \left[1 + 0.4\eta^+ \left(1 - \exp\left(-(\eta^+/L)^2\right) \right) \right], \quad \eta^+ = zu_{*0}/\nu_a$$

Here $L = 22.4$, $\nu_a = 0.15 \text{ cm}^2/\text{s}$ is the kinematical viscosity of the air.

[10] We estimated the hydrodynamic and RCS contrasts in the field of orbital velocities U_w corresponding to measurements of sea surface elevation in the tsunami wave of 26 December 2004 provided by Jason-1. According to the long wave theory $U_w = c\eta_0/H$, where $H = 4000$ m is the depth of the ocean, $c = 200$ m/s is the tsunami wave velocity, η_0 is the displacement of the sea level taken from GDR.

[11] The problem (2a)(2b) was solved by the method of the Fourier decomposition in time variable. For each single harmonic the scale of the unsteady boundary layer in the airflow, $\delta_{ts} = \kappa u_{*0}/\omega$. If δ_{ts} significantly exceeds the scale of the viscous sub-layer $\delta_{wave} = (20 \div 30) \nu_a/u_{*0}$, then near the water surface the wind velocity profile is logarithmic:

$$U(\eta) = u_{*0}/\kappa \ln(\eta/z_*) + U_{w0} e^{-i\omega(t-x/c)} + \Delta u,$$

where the roughness parameter, $z_* = 0.11 \nu_a/u_{*0} \exp(-\kappa \Delta u/u_{*0})$ are modulated with the tsunami wave period. Here $\Delta u = \int_0^\infty \tau_{wave}/\nu_a d\eta_1 < 0$ is the negative non-linear addition to the wind velocity caused by the momentum flux from wind to waves. If the wind friction velocity disturbance, u_{*1} , caused by the tsunami wave, is small ($|u_{*1}| \ll u_{*0}$), then solution to (2) gives

$$u_{*1} = \kappa U_{w0} \left(\ln \left(3.178 \omega \nu_a 0.11 / \kappa u_{*0}^2 \right) - 1 - \frac{\partial \Delta u}{\partial u_{*0}} \Big|_{u_{*0}=u_{*0}} + \pi i/2 \right)^{-1}.$$

[12] Near the stability threshold the amplitudes of disturbances obey the Landau-Stewart equation [see *Craik*, 1986]. For wind water waves it is as follows:

$$s_t = \left(\frac{\partial \beta}{\partial u_{*0}} \Big|_{u_{*0}=u_{*c}} \right) (u_{*0} - u_{*c}) s - s |s|^2 \gamma \quad (3)$$

Here s is the slope of the most unstable disturbance with the wave number $k = k_c$, $|s|^2 \gamma$ is the nonlinear addition to the wind growth rate and the viscous decrement. The nonlinear wind-wave interaction causes generation of the induced flow in the air. Outside the short-wave boundary layer it is reduced to nonlinear addition to the wind velocity Δu , near the stability threshold $\Delta u = -u_{*0} \delta |s|^2$. Numerical calculations within the model of a turbulent boundary layer over the waved water surface developed by *Reutov and Troitskaya* [1995] give, $k = k_c \approx 1 \text{ cm}^{-1}$, $u_{*c} = 4.95 \text{ cm/s}$, $\frac{\partial \beta}{\partial u_{*0}} \Big|_{u_{*0}=u_{*c}} = 0.0122 \text{ cm}^{-1}$, $\gamma = 1.09 \text{ c}^{-1}$, $\delta = 241$. Since the time scale of the tsunami wave, 10^3 c , significantly exceeds the scale of growth of the short surface waves, then the slope can be determined as a stationary solution to equation (3): $|s|^2 = \frac{\partial \beta}{\partial u_{*0}} \Big|_{u_{*0}=u_{*c}} (u_{*0} - u_{*c}) / \gamma$, $\Delta u = -\frac{\partial \beta}{\partial u_{*0}} \Big|_{u_{*0}=u_{*c}} (u_{*0} - u_{*c}) u_{*0} \delta / \gamma$. This calculations are valid within applicability of the weakly nonlinear asymptotic model, i.e., for $|s| \ll 1$. If we take $|s|^2 < 0.02$, then $(u_{*0} - u_{*c}) < 0.01 \gamma / \frac{\partial \beta}{\partial u_{*0}} \Big|_{u_{*0}=u_{*c}} \approx 2$; that is, the model is applicable for $u_{*0} < 7 \text{ cm/s}$.

[13] For a narrow spectra realized near the stability threshold $|s|^2$ is proportional to the slope spectrum at $k =$

k_c . Then the hydrodynamic spectral contrast $C(k_c)$ of variations of the surface wave intensity for $k = k_c$ can be estimated as $C(k_c) = \Delta|s|^2/|s|_0^2 = u_{*1}/(u_{*0} - u_{*c})$, where $\Delta|s|^2$ is the variation of the slope caused by variations of the wind friction velocity. Expressions for u_{*1} and Δu give

$$C(k_c) = \kappa U_{w0} (u_{*0} - u_{*c})^{-1} \left(\ln \left(3.178 \omega \nu_a 0.11 / \kappa u_{*0}^2 \right) - 1. + Q(2u_{*0} - u_{*c}) / u_{*c} + \pi i / 2 \right)^{-1}, \quad (4)$$

where $Q = \kappa u_{*c} \delta \partial \beta / \partial u_{*c} |_{u_{*c} = u_{*c} / \gamma} = 5.38$.

[14] The dependencies of the module and phase of $C(k_c)$ on u_* are presented in Figure 5 for the orbital velocity in the tsunami wave 2.25 cm/s and frequency 0.007 s⁻¹, corresponding to the local elevation of the water surface near the equator (see Figure 2a). For the 10-meter wind velocity $U_{10} = 2-3$ m/s u_* is approximately 6–7 cm/s [see, e.g., Miles, 1962]. Then modulus C is approximately 0.2, and phase is close to π . It means, that under fair wind conditions elevation of the water surface in the tsunami wave is accompanied by reducing of the wind ripples and increasing RCS that is in agreement with Figure 2a. The hydrodynamic contract of the ripples in the velocity field (2) can be calculated by the Fourier transformation of (4).

[15] Let us now relate the variations in the spectrum of short wind waves due to tsunami with variations of RCS. According to the composite model of scattering the nadir RCS can be written as $\sigma_0 = R_{eff} / 2s_u s_c$, where $R_{eff} = |R(0)|^2 \exp(-4k_r^2 \langle h_s^2 \rangle)$, $R(0)$ is the Fresnel reflection coefficient at normal incidence, k_r radar wave number, $\langle h_s^2 \rangle$ is the mean squared height of short wind waves (smaller than approximately 3 times the radar wavelength), s_u, s_c the RMS long wave slopes in along and crosswind directions, respectively [see, e.g., Anderson et al., 2002, and references therein]. Under weak wind conditions for Ku band it easily follows from the expression for σ_0 , that $\Delta \sigma_{0Ku} = -C_{hydro}$. These theoretical estimations are in a good agreement with $\Delta \sigma_{0Ku}$ calculated by the empirical dependence (1) using the data set of GDR (see Figure 6).

[16] It is important to emphasize, that the tsunami orbital velocity is approximately 2.5 cm/s and the wind velocity is about 2–3 m/s. It means, that in the presence of tsunami, wind velocity varies on 1% from the background value. Such small wind velocity variations can result in substantial variation of the RSC (about 1dB), under special conditions of weak wind, when the variable component of the drag of the sea surface is mainly supported by variations of momentum flux to short wind waves. It could be explained by combination of a number of factors. In fact, the addition to the wind velocity, induced in the air by the orbital velocity of the tsunami, is not homogeneously spread over the

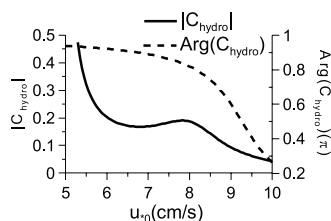


Figure 5. Amplitude and phase of the hydrodynamic contrast.

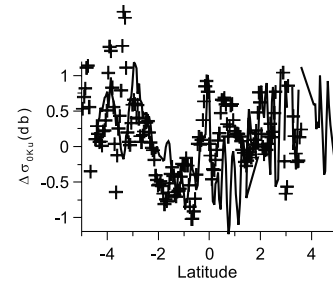


Figure 6. Comparison of the measured C-band RCS and the theoretical estimation. Here crosses are the C-band RCS taken from the GDR of Jason-1, where large-scale background variations in the domain between -5° and 5° are subtracted. Line is the theoretical estimations.

boundary layer, but it has the maximum near the water surface (in the domain of short-wave-wind energy exchange). Besides, strong nonlinear wave-wind interaction near the stability threshold (i.e., large coefficients of nonlinear interaction) leads to the strong “feed-back effect” [see Kudryavtsev et al., 1997]. At last, under the conditions of the weak wind the threshold effect is expected to enlarge the hydrodynamic and radar contrast.

[17] Thus, there is both an unambiguous experimental evidence of observation from space of tsunami in the open ocean through variations of radar cross-section in phase with the water elevation and a plausible mechanism explaining the effect. To decide on the perspectives of this finding for tsunami monitoring and, possibly, tsunami warning systems the following points should be taken into consideration. On one hand, the effect was observed under favorable conditions of weak wind and large tsunami wave amplitude, when high hydrodynamic contrasts of short surface waves are expected. On the other hand, it was an observation “by chance”, performed by an instrument, which was not designed for measurements of the sea roughness. It is expected, that the use of special algorithms of coherent signal processing (for example, image recognition) and optimal filtering could strongly enhance contrasts of tsunami images in the open ocean even at much less favorable conditions.

[18] **Acknowledgments.** We are grateful to V. Shrira for stimulating conversations on the problem of tsunami remote sensing and valuable advices concerning the manuscript and to A. V. Gaponov-Grekhov for helpful discussions on possible mechanisms of short wave modulation in the presence of a tsunami wave. We thank G. Balandina for the help with data processing. We are grateful to the anonymous reviewers for valuable comments, which helped us to improve the manuscript. This work was supported by grants from RFBR (project 05-05-64137).

References

- Alpers, W. (1985), Theory of radar imaging of internal waves, *Nature*, 314, 245.
- Anderson, C., J. Trevor, C. D. Gommenginger, and M. Srocosz (2002), A comparison of the sea-state sensitivity in empirical and theoretical models of altimeter ocean backscatter, *Can. J. Remote Sens.*, 28, 475.
- Craik, A. (1986), *Wave Interactions and Fluid Flows*, Cambridge Univ. Press, New York.
- Godin, O. A. (2004), Air-sea interaction and feasibility of tsunami detection in the open ocean, *J. Geophys. Res.*, 109, C05002, doi:10.1029/2003JC002030.
- Gower, J. (2005), Jason 1 detects the 26 December 2004 Tsunami, *Eos Trans. AGU*, 86(4), 37.

- Kudryavtsev, V. N., C. Mastenbrock, and V. K. Makin (1997), Modulation of wind ripples by long surface waves via the air flow: A feedback mechanism, *Boundary Layer*, *83*, 99.
- Kulikov, E. (2005), Analysis of satellite altimetry observations during the Sumatra Tsunami of December 26, 2004, *Geophys. Res. Abstr.*, *7*, Abstract 11063.
- Lay, T., et al. (2005), The Great Sumatra-Andaman Earthquake of 26 December 2004, *Science*, *308*, 1127.
- Miles, J. W. (1962), On the generation of surface waves by shear flows. part 4, *J. Fluid Mech.*, *13*, 433.
- Okal, E. A., A. Piatanesi, and P. Heinrich (1999), Tsunami detection by satellite altimetry, *J. Geophys. Res.*, *104*, 599.
- Picot, N., K. Case, S. Desai, and P. Vincent (2003), *AVISO and PODAAC User Handbook*, Aviso, Ramonville St-Agne, France.
- Reutov, V. P., and Y. I. Troitskaya (1995), On nonlinear effects due to water wave interaction with turbulent wind, *Izv. Russ. Acad. Sci., Atmos. Oceanic Phys.*, *31*, 825.
- Scharroo, R., W. Smith, V. Titov, and D. Arcas (2005), Observing the Indian Ocean tsunami with satellite altimetry, *Geophys. Res. Abstr.*, *7*, Abstract 09407.
- Smolyakov, A.V. (1973), The spectrum of the quadruple radiation of the plane turbulent boundary layer, *Acoust. J.*, *19*, 420.
- Troitskaya, Y.I. (1994), Modulation of the growth rate of short surface capillary-gravity wind waves by a long wave, *J. Fluid Mech.*, *273*, 169.
- Zaychenko, M., E. Kulikov, B. Levin, and P. Medvedev (2004), *Examples of Offshore Tsunami Registration According to Satellite Altimeter Data (1993–2001)*, Yanus-K, Moscow.

S. A. Ermakov and Y. I. Troitskaya, Institute of Applied Physics, Russian Academy of Sciences, U'lyanov str., 46, 603950 Nizhny Novgorod, Russia. (yuliya@hydro.appl.sci-nnov.ru)